Article

Chemistry & Biology

A Potassium Ion-Dependent RNA Structural Switch Regulates Human Pre-miRNA 92b Maturation

Graphical Abstract

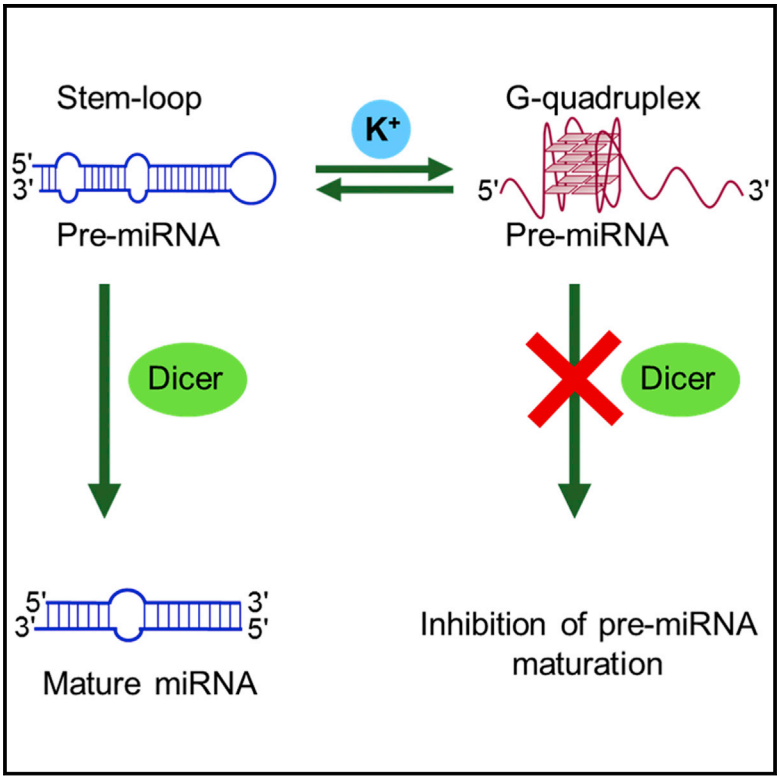

Highlights

- About 16% of human pre-miRNAs contain putative G-quadruplex (GQ) forming sequences
- Formation of GQ unwinds the canonical stem-loop structure of human pre-miRNA-92b
- GQ structure of pre-miRNA 92b coexists with stem loop in the presence of 100 mM K^+
- GQ inhibits Dicer-mediated maturation of pre-miRNA 92b both in vitro and in vivo

Authors

Gayan Mirihana Arachchilage, Arosha C. Dassanayake, Soumitra Basu

Correspondence

sbasu@kent.edu

In Brief

G-quadruplex (GQ) structure regulates the maturation of human pre-miRNA 92b. Mirihana Arachchilage et al. describe the formation of GQ as an alternative to the canonical stem-loop structure and show that the GQ formation inhibits Dicer-mediated maturation of pre-miRNAs.

Mirihana Arachchilage et al., 2015, Chemistry & Biology *22*, 262–272
February 19, 2015
http://dx.doi.org/10.1016/j.chembiol.2014.12.013

CellPress

CellPress

Chemistry & Biology
Article

A Potassium Ion-Dependent RNA Structural Switch Regulates Human Pre-miRNA 92b Maturation

Gayan Mirihana Arachchilage,[1] Arosha C. Dassanayake,[1] and Soumitra Basu[1,*]
[1]Department of Chemistry and Biochemistry, Kent State University, Kent, OH 44242, USA
*Correspondence: sbasu@kent.edu
http://dx.doi.org/10.1016/j.chembiol.2014.12.013

SUMMARY

MicroRNAs (miRNAs) are an important set of oligonucleotide sequences with a biogenesis that involves Dicer-mediated cleavage as a critical step. Dicer cleaves the precursor miRNA (pre-miRNA) stem-loop structure to produce the mature miRNA. Using bioinformatics analysis, we discovered the presence of putative G-quadruplex (GQ)-forming sequences in about 16% of pre-miRNAs. We report the existence of a GQ as an alternative to the canonical stem-loop structure in the clinically important human pre-miRNA 92b. GQ formation led to unwinding of the stem-loop structure imparting resistance to Dicer-mediated cleavage both in vitro and in vivo. A potential K^+ ion-dependent equilibrium between GQ and the stem-loop structure has the ability to regulate the Dicer-mediated maturation of pre-miRNA 92b, which consequently affects target gene silencing. These findings unravel a new mechanism of regulation in pre-miRNA maturation, albeit at the RNA structure level.

INTRODUCTION

MicroRNAs (miRNAs) are endogenous short RNA sequences (~22 nucleotides) that regulate expressions of more than one-half of the human protein coding genes (Bartel, 2004; Friedman et al., 2009). The genes that encode miRNAs are transcribed by RNA polymerase II or III, and these transcripts adopt a long hairpin-like structure termed primary miRNA (pri-miRNA) (Borchert et al., 2006; Lee et al., 2004). A microprocessor complex containing an RNase III enzyme, Drosha, and DiGeorge critical region 8 (DGCR8) protein cleaves the pri-miRNA hairpin stem to generate the precursor miRNA (pre-miRNA), which adopts a stem-loop structure (Denli et al., 2004; Lee et al., 2003). Alternatively, some pre-miRNAs named mirtrons are directly spliced out from host genes bypassing the Drosha-mediated cleavage (Ruby et al., 2007; Sand, 2014). In the cytoplasm, the enzyme Dicer belonging to the RNase III family cleaves the pre-miRNA stem loop to produce mature miRNAs, which are eventually loaded onto the RNA-induced silencing complex (Bernstein et al., 2001; Hutvágner et al., 2001; Winter et al., 2009). Thus, Dicer-mediated miRNA cleavage is a critical step in miRNA biogenesis as it regulates the mature miRNA levels in cells that are often linked with different disease conditions, including cancer (Di Leva et al., 2014; Hesse and Arenz, 2014; Winter and Diederichs, 2011).

The stem-loop structure is a characteristic of pre-miRNAs and contains internal loops, short overhangs, mismatches, and bulges (Griffiths-Jones, 2004; Krol et al., 2004). The double-stranded stem loop is critical for Dicer-mediated maturation of pre-miRNAs as the enzyme is known to recognize the double-stranded ends via its PAZ domain (MacRae et al., 2007). It has been shown that the different domains of human Dicer enzyme act coordinately to recognize and cleave the pre-miRNA stem loops and produce mature miRNA duplex (Ma et al., 2012). Dicer cleavage site is known to be determined by the features of the stem-loop structures. It has been illustrated that Dicer measures a fixed distance from either 5′ phosphate group (5′ counting rule) or 3′ overhang (3′ counting rule) to determine the cleavage site (MacRae et al., 2007, 2006; Park et al., 2011). In addition, Dicer also recognizes the loop/bulge structure of pre-miRNAs for accurate processing (loop counting rule) (Gu et al., 2012). Human Dicer tolerates a significant amount of structural variations in stem-loop characteristics, such as mismatch-containing stem, large end loop, and 3′ overhang, which favor the pre-miRNA cleavage (Feng et al., 2012). The current dogma solely takes into account the fact that all the pre-miRNAs adopt stem-loop structures that are critical for Dicer-mediated maturation and thus alternative secondary structures are not actively considered. However, after a comprehensive sequence analysis of all the pre-miRNAs, we discovered that many human pre-miRNAs contain guanosine (G)-rich regions, some of which overlap with the corresponding mature miRNAs. Therefore, we proposed that these G-rich regions can adopt G-quadruplex (GQ) structures as an alternative to the canonical stem-loop structure. Since the Dicer enzyme is considered to be stem-loop structure specific, GQ formation may act as an impediment to the Dicer-mediated cleavage.

We have elucidated the potential regulatory role of the noncanonical GQ secondary structure in the Dicer-mediated maturation of a human pre-miRNA that results in the clinically important miRNA 92b (hsa-mir-92b). The human miRNA 92b is significantly upregulated in non-small-cell lung cancer (NSCLC) and it is involved in the development of drug resistance in NSCLC (Li et al., 2013). Increased miRNA 92b expression in glioblastomas makes it function as a potential oncogene via targeting of the Smad3 (Wu et al., 2013). It is also specifically expressed in

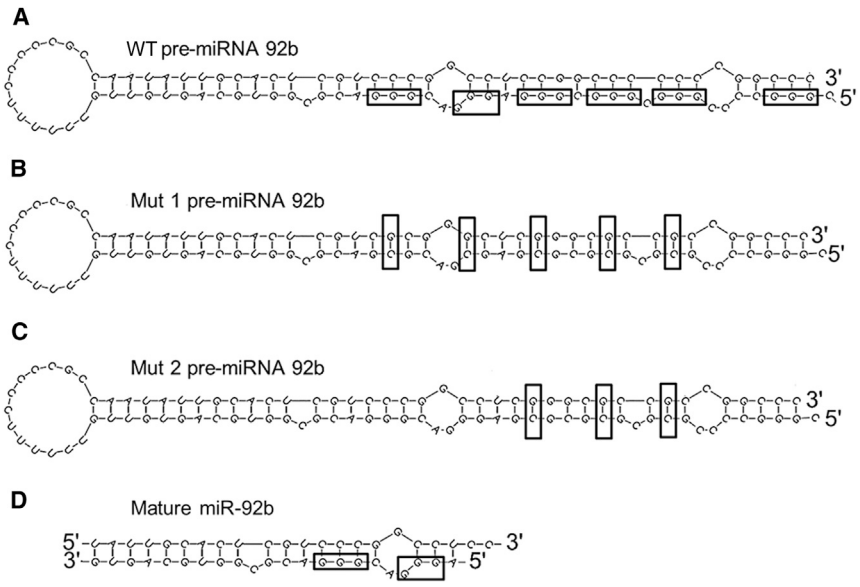

Figure 1. Pre-miRNA 92b Contains Putative GQ Forming Sequence (PQS)

(A–D) Predicted stem-loop structure for (A) WT pre-miRNA 92b, (B) Mut 1, (C) Mut 2, and (D) mature miR-92b. G tracts in the PQS region and swapped base pairs are boxed. See also Tables S1 and S2.

primary brain tumors and can potentially be used to differentiate primary from metastatic brain tumors (Nass et al., 2009). In addition, miRNA 92b controls the G1/S checkpoint gene *p57* in human embryonic stem cells (Sengupta et al., 2009). Human pre-miRNA 92b contains six stretches of 3Gs, raising the potential for robust GQ formation. RNA molecules can coexist as a GQ and a hairpin structure under the physiologically relevant salt concentrations (Bugaut et al., 2012). GQ structures are formed by stacking of two or more square planar structures known as G-quartets and are stabilized by monovalent cations, particularly potassium (Campbell and Neidle, 2012). G-quartets are formed by four consecutive G stretches of two or more Gs in each stretch and are often found in G-rich regions (Neidle and Balasubramanian, 2006). GQs are widespread in various types of RNAs, including mRNA, long noncoding RNA, telomeric RNA, and viral genomic RNA, and have been shown to play vital roles in RNA biology (Kumari et al., 2007; Arora et al., 2008; Jayaraj et al., 2012; Martadinata and Phan, 2013; Millevoi et al., 2012; Sundquist and Heaphy, 1993). Using different biochemical and biophysical approaches, we unraveled the role of GQ formation in the maturation of human pre-miRNA 92b. The findings reported here will broaden our understanding about the mechanism of Dicer-mediated maturation at the pre-miRNA structural level and add a new layer to the set of regulations in miRNA biogenesis.

RESULTS

In Silico Analysis Identified a Large Number of Putative GQ Sequences in Pre-miRNAs

We investigated putative GQ sequences (PQSs) that are found in human pre-miRNAs via in-house analysis using QGRS mapper (a GQ structure prediction software) (Kikin et al., 2006). It is well known that DNA or RNA sequences that contain $G_{2-5}N_{1-7}G_{2-5}N_{1-7}G_{2-5}N_{1-7}$ G_{2-5} can adopt GQ structures, where N can be any nucleotide (Kikin et al., 2006). We discovered that of 1881 human pre-miRNA sequences published in the miRNA database (http://www.mirbase.org, release 21: June 2014), 298 pre-miRNAs contained PQS with high predictive scores (G score $\geq$30); the top 50 from that list are shown in Table S1 (Griffiths-Jones et al., 2008). Furthermore, we investigated the location of the GQ in the pre-miRNAs. We found that the GQs are present in the passenger strand, guide strand, and outside the mature miRNAs. However, the majority of the miRNAs are not fully characterized and the guide and passenger strands are not accurately identified. Thus, it was not possible to detect any pattern of the location of the GQs. Given that the canonical stem-loop structures are universally present in the known pre-miRNAs, the discovery of the existence of PQSs led us to rationalize that in those pre-miRNAs the GQ can potentially be an alternative structure, which may remain in equilibrium with the stem-loop and affect Dicer-mediated maturation.

Human Pre-miRNA 92b Contains a Conserved Putative GQ Forming Region

Human miRNA 92b is one of the clinically important miRNAs found among the above-mentioned set of G-rich pre-miRNAs and is one of the top 20 potential disease-related miRNAs (Chen and Yan, 2014). Pre-miRNA 92b is 96 nucleotides long and can adopt a characteristic stem-loop structure that was confirmed by mfold structure prediction software (Figure 1A) (Zuker, 2003). According to the miRNA database, both 3p-miR-92b and 5p-miR-92b strands of the mature miRNA 92b duplex (miR-92b) are 22 nucleotides (nt) long (Figure 1D) (Griffiths-Jones et al., 2008). Pre-miRNA 92b has six G stretches, each containing three Gs, which are located 2–28 nucleotides from the 5′ end (Figure 1A). This region can be recognized as a PQS, as it fits to the $G_{2-5}N_{1-7}G_{2-5}N_{1-7}G_{2-5}N_{1-7}$ G_{2-5} formula. Using QGRS mapper multiple overlapping, PQSs were found with high G scores (highest G score 62, Table S2), indicating its ability to adopt stable GQ structures (Kikin et al., 2006). As a reference, using the same set of parameters, we analyzed two well-characterized and very stable GQs found in the 5′ UTRs of MT3-MMP and NRAS mRNAs and in both cases the G score turned out to be 60, indicating that the PQS in pre-miRNA 92b (G score 62) can form a very stable GQ structure (Kumari et al., 2007; Morris and Basu, 2009). Identical or very similar type of three-tier PQSs were found to be conserved among pre-miRNA 92b of several species, such as Chinese hamster, cattle, mouse, and many others, including some of the primates (Table S2). Putative quadruplex forming sequence and its complementary strand cover about one-half the length of the human miRNA 92b stem loop and therefore GQ formation can potentially destabilize the

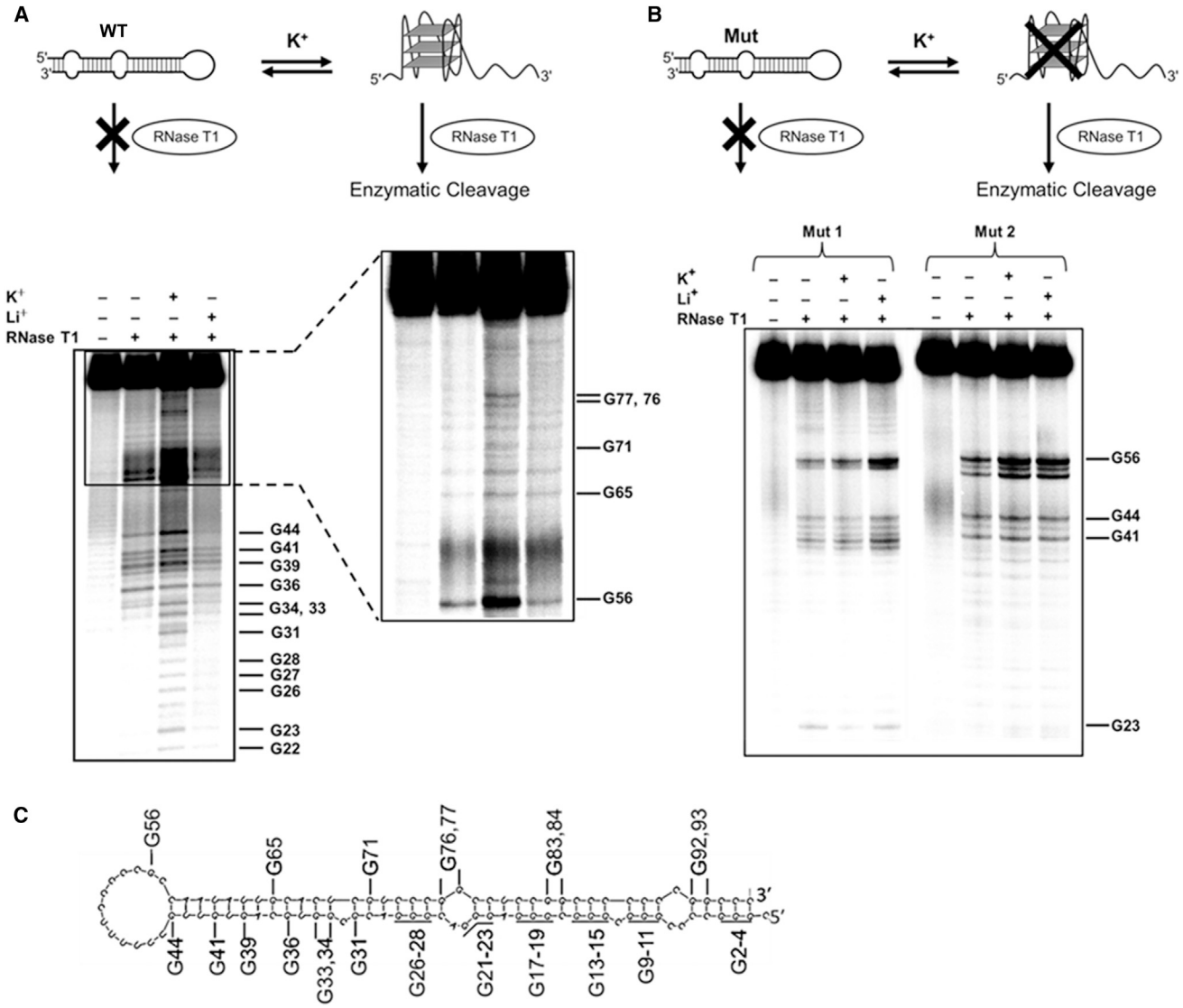

Figure 2. GQ Formation Unwinds the Canonical Stem-loop Structure of Pre-miRNA 92b

(A) RNase T1 structure mapping of WT shows that the stem-loop structure unwinds in the presence of 100 mM K^+ but not with 100 mM Li^+. The enlarged panel was obtained by running the same samples for a longer time. The bands were assigned according to a base hydrolysis ladder. The entire gel image is shown in Figure S1.

(B) RNase T1 structure mapping of Mut 1 and Mut 2, indicating that the stem-loop structure does not unwind under any salt condition due to the inability to form the GQ.

(C) Mfold predicted stem-loop structure of pre-miRNA 92b with numbered G residues.

(A) and (B) follow the numbering shown in (C). See also Figure S1.

stem-loop structure. Thus, we hypothesized that if GQ structure forms in the presence of K^+, the canonical hairpin structure would unwind.

Formation of GQ Structure Unwinds the Canonical miRNA 92b Stem Loop

To investigate the stem-loop unwinding of pre-miRNA 92b due to the formation of GQ structure, RNase T1 structure mapping was performed. Guanosines (G) that are involved in either stem regions or GQ structures are known to be protected from the RNase T1 enzymatic cleavage (Aldaz-Carroll et al., 2002; Darnell et al., 2001; Morris and Basu, 2009). The data showed that in the absence of K^+, most of the Gs were protected except the G in the hairpin loop (G56), indicating that the pre-miRNA 92b exists as a canonical stem-loop structure (Figure 2A). Gs close to the hairpin loop (G36 to G44) were slightly less protected compared with the other Gs, which may be due to their involvement in relatively weaker wobble base pairing. In the presence of 100 mM K^+, almost all of the Gs that were protected in the absence of K^+ underwent some level of cleavage, indicating the unwinding of the pre-miRNA stem-loop structure, most likely due to formation of the GQ, which enabled RNase T1 to have increased access to

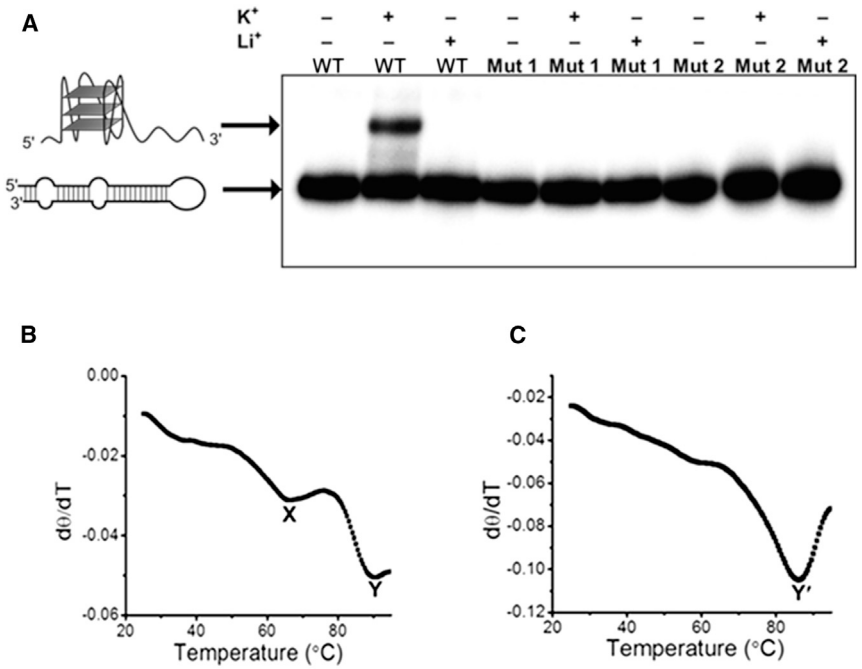

Figure 3. Pre-miRNA 92b Coexists as GQ and Stem-loop Structures in the Presence of K^+

(A) Gel mobility shift assay shows the coexistence of two structures in the presence of 100 mM K^+. A less compact structure was observed only with WT pre-miRNA 92b in the presence of 100 mM K^+ but not with Mut 1 or Mut 2, indicating the GQ structure formation causes the unwinding of the stem loop. See also Figures S2 and S3.

(B and C) First derivative of a representative CD melting curve of WT (B) and Mut 2 (C) at a 2.5 μM RNA concentration in 10 mM Tris, 0.1 mM EDTA, and 5 mM K^+. WT showed two distinct melting points (X = 63.5 ± 1.7°C and Y = 90.0 ± 0.5°C), whereas Mut 2 showed only a single melting point (Y' = 86.0 ± 0.9°C). The average melting temperatures were calculated from three independent experiments (± SEM, n = 3). See also Figure S4.

the Gs. The observation that Gs that are in the PQS (G2 to G28) were protected even in the presence of K^+ compared with the Gs in the other regions implied the formation of GQ structure (Figure 2A; Figure S1). To further assess if the stem-loop unwinding is due to the formation of the GQ, RNase T1 structure mapping was performed in the presence of 100 mM of Li^+. Lithium (I) is known to disfavor the GQ formation, but it should not adversely affect the stability of the stem-loop structure. The data showed that most of the Gs were found to be protected in the presence of 100 mM Li^+ and the pattern of protection was identical to the pattern observed in the absence of K^+, which is due to lack of GQ formation, which allowed the maintenance of the stem-loop structure. Based upon the above observations, we can conclude that the unwinding of the canonical stem-loop structure in the presence of K^+ is due to the formation of GQ.

To confirm further that the adoption of GQ conformation causes the stem-loop unwinding of pre-miRNA 92b, two of its mutant versions (Mut 1 and Mut 2) were designed (Figures 1B and 1C). Both Mut 1 and Mut 2 were designed to completely eliminate the intramolecular GQ formation, while maintaining the stem-loop structure intact. However, Mut 2 was designed in such a fashion as to produce a mature sequence that is very similar to the wild-type (WT) pre-miRNA 92b. The mutations were effected by swapping positions of selected Gs within the PQS region with the corresponding cytosines (Cs) of the complementary strand to maintain the same base paring and the duplex structure but disrupt the GQ formation. Overall, the stem-loop structures of the Mut 1 and Mut 2 were confirmed to be similar to the WT by the mfold structure prediction program (Figures 1B and 1C) (Zuker, 2003). RNase T1 structure mapping was also performed on the mutants under identical conditions at which the WT sequence was treated. All the Gs except those inside or close to the terminal loop (G56, G44, and G41) were protected from the enzymatic cleavage regardless of the salt condition (Figure 2B). G23 was slightly cleaved, as it is in the internal loop. These data indicate that the canonical stem-loop structure remains intact even in the presence of K^+ if the PQS is altered in such a way so as to eliminate the possibility of intramolecular GQ formation. Collectively, these results establish that the formation of GQ can unwind the entire canonical stem-loop structure of pre-miRNA 92b in the presence of physiologically relevant K^+ concentration.

In the Presence of K^+ Pre-miRNA 92b Coexists as the Canonical Stem-loop and GQ Structures

The existence of the noncanonical pre-miRNA GQ structure was further investigated using a gel mobility shift assay. The WT and the two mutant RNAs were folded in the presence of K^+, Li^+, or with no added salt, and the structures were analyzed by native PAGE. In the absence of salt and in the presence of Li^+, only a faster migrating band was observed, which should correspond to the canonical stem-loop structure (Figure 3A). In addition to the species described above, a slower migrating band of WT pre-miRNA was also observed in the presence of K^+. This slower migrating species, which was observed only in the presence of K^+, is expected to be less compact than the stem loop and it most likely is the GQ structure, with the remainder of the sequence being in an unfolded form. Although the GQs are typically compact structures, in this case, as a whole, the molecule containing the GQ should be less compact than the stem loop, due to its long unstructured flanking region (about 60–68 nt long) toward the 3′ end. Moreover, for the mutant RNAs that lack the PQS, only the band corresponding to the stem-loop structure was observed under all of the conditions that were tested, including in the presence of K^+, indicating that the GQ formation is required to unwind the stem loop. These results reveal the coexistence of GQ structure with the canonical stem loop in the presence of physiologically relevant K^+ concentration. Furthermore, we confirmed that the cytoplasmic Mg^{2+} concentration has no effect on structural coexistence of pre-miRNA 92b, which was observed in the gel mobility shift assay (Figure S2). Although Figure 3A indicates that the population of the

stem-loop structure is higher than that of the GQ, when the RNA was folded at 37°C for 20 min, we observed that the equilibrium shifted more toward the GQ structure (Figure S3). However, more detailed experiments are needed to evaluate the folding kinetics of the two structures in the presence of K^+ ions. Collectively, these results indicate that pre-miRNA 92b may exist as an equilibrium between the GQ and the stem-loop structure in the cytoplasm, and the elimination of the GQ forces the equilibrium toward the stem-loop structure, which led us to conclude that the equilibrium may regulate the Dicer-mediated maturation of miRNA 92b.

To further assess the coexistence of GQ and the stem-loop structures of pre-miRNA 92b, WT and Mut 2 RNAs were folded in the presence of 5 mM K^+ and subjected to thermal melting, which was monitored by circular dichroism (CD) spectroscopy (Figure S4). Two distinct melting points were observed for the WT, as shown in the first derivative of the melting curve (Figure 3B). However, only one melting point was observed when the Mut 2 was melted in 5 mM K^+ (Figure 3C). Therefore, the additional melting point (labeled as X in Figure 3B) that was observed for the WT most likely corresponds to the melting of the GQ structure, as it was absent in the Mut 2 melting profile (Figure 3C). Melting points observed in both WT and Mut 2 (*Y* and *Y′*, respectively [Figures 3B and 3C]) should correspond to the melting of the stem loop, which also generated a positive peak at 260 nm in the CD spectrum of the duplex (Kypr et al., 2009). We also observed that both WT and Mut 2 generate 260 nm positive peaks in CD spectra (data not shown). Interestingly, both WT and the Mut 2 showed close melting temperatures (T_m) for the stem loop (*Y* = 90.0 ± 0.5°C and *Y′* = 86.0 ± 0.9°C), indicating that the base swapping in Mut 2 essentially did not change the stability of the stem-loop structure. The melting temperature of the GQ (*X*) was found to be 63.5 ± 1.7°C, which matches with the T_m values for three-tier GQs reported in the literature (Kumari et al., 2007; Morris and Basu, 2009). At 100 mM K^+, we did not observe any melting that could be assigned to the GQ structure (data not shown). Based upon previous reports from our laboratory and others, this was not unexpected, as GQs of such stability failed to undergo thermal melting in presence of 100 mM K^+ (Morris and Basu, 2009; Zhang et al., 2011).

Chemical and Enzymatic Structure Mapping Confirmed the Switch to a GQ Structure

To further confirm that the additional structure found in the gel mobility shift assay is a GQ, dimethyl sulfate (DMS) structure mapping was performed on the WT RNA. DMS methylates G if the N7 position is not engaged with a bond and thus can be used specifically to probe the GQ structure (Morris et al., 2010; Neidle and Balasubramanian, 2006). If the molecule is in the form of stem loop, the Gs can be modified by the DMS, as the N7 position is not used in Watson-Crick base pairing. In contrast, the Gs that are involved in the GQ will be protected from the DMS modification, because the N7 positions are used in the Hoogsteen base paring in the context of a G tetrad. When the WT RNA was folded in the presence of 100 mM K^+, Gs that are in the PQS region (G23 to G9) were protected from the cleavage compared with the RNAs folded in the presence of 100 mM Li^+ or without any added salt (Figure 4A). This salt-dependent protection is direct evidence of the GQ formation over the duplex structure by the pre-miRNA 92b in the presence of 100 mM K^+. The Gs that are not involved in the GQ formation (G33 to G65) are not protected under any salt condition. Few of the Gs (G26, G27, G28, and G31) are protected in all of the lanes, which is obviously due to the lack of accessibility, but finding the reasoning behind the observation will require high-resolution structural data.

In a separate experiment, we subjected the pre-miRNA 92b sequence to RNase T1 structure mapping with increased (5-fold excess compared with the previous studies) enzyme concentration and observed that all the Gs were cleaved even in the absence of K^+. The data indicate that the stable stem-loop structure starts to undergo cleavage at high RNase T1 concentration (Figure 4B). Interestingly, in the presence of K^+ and the high enzyme concentration, Gs that are in the PQS were still protected from the RNase T1 cleavage, which is in contrast to the observation made in the absence of K^+, where all Gs were cleaved, suggesting that the duplex structure breathes more compared with the GQ. The results discussed above further confirm that the Gs in the PQS participate in GQ structure formation.

GQ Structure Formation Inhibits Dicer-Mediated Maturation of Pre-miRNA 92b In Vitro

The stem loop is required for miRNA maturation, as Dicer is known to recognize only double-stranded RNAs and cleaves them to form mature miRNA duplexes. Since a non-stem-loop structure containing a GQ was observed for pre-miRNA 92b, we rationalized that this noncanonical structure should impede Dicer-mediated cleavage at the physiological K^+ concentration. To test this hypothesis, an in vitro Dicer assay was performed on body labeled ([α-^{32}P]CTP) pre-miRNA 92b using human recombinant Dicer enzyme. Analysis of the Dicer cleaved WT showed more of the 22-nt-long matured product (labeled with *) in the absence of K^+ compared with the amount in the presence of 100 mM K^+ (Figure 5A). This indicates that the Dicer-mediated cleavage is most likely impaired by the formation of GQ structure. When the same concentration of Li^+ was used to disfavor the GQ formation, cleavage was determined to be at a level similar to that observed in the absence of K^+. Thus, the pre-miRNA 92b undergoes the same amount of Dicer-mediated cleavage at both 100 mM Li^+ and in the absence of K^+, leading to the conclusion that the lower amount of cleavage in 100 mM K^+ was due to GQ formation and not an ancillary effect because of the extra monovalent metal ions.

To further confirm that the GQ formation affects the Dicer-mediated cleavage, Mut 2 (Figure 1C) was utilized because the maturation of this sequence is expected to result in a similar product to the mature miRNA-92b; however, it cannot adopt a GQ. Both WT and Mut 2 versions of pre-miRNA 92b were subjected to Dicer-mediated cleavage in the presence of 100 mM K^+ and in the absence of any added salt. Mut 2 showed a similar amount of maturation of pre-miRNA92b in the absence and the presence of K^+, indicating that there is no difference in the action of Dicer on the molecule because the stem-loop structure is maintained regardless of the salt concentration, as was established earlier in our study (Figure 5B). In contrast, a significant difference in band intensities was observed in the cleavage of the

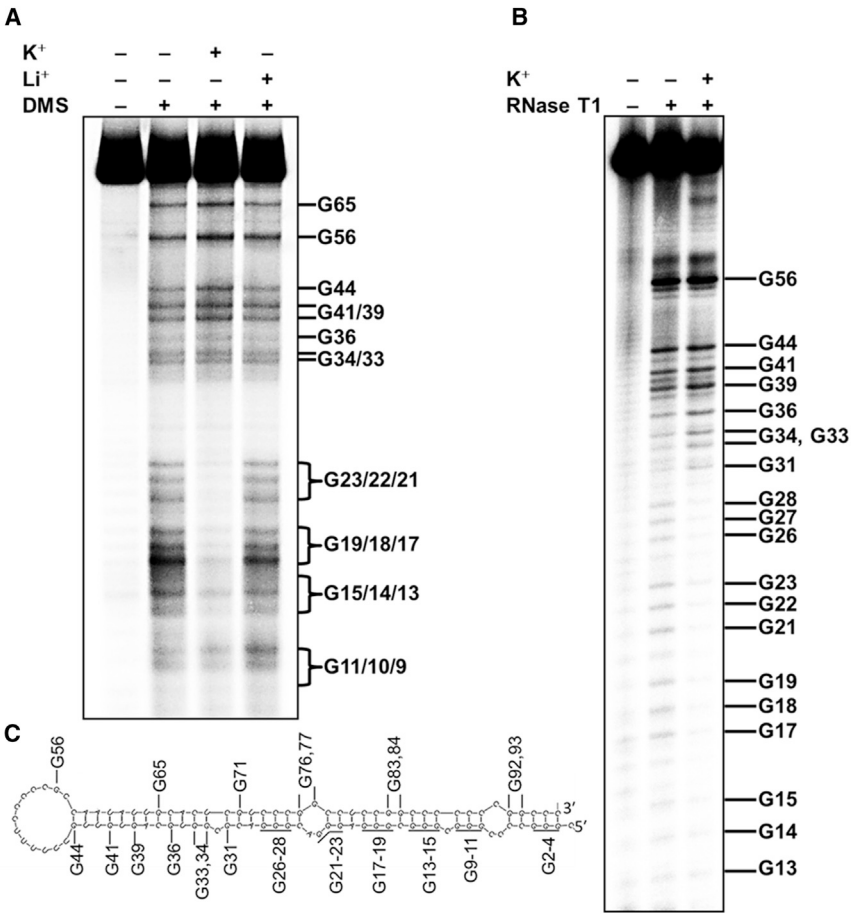

Figure 4. Chemical and Enzymatic Structure Mappings Show the Formation of GQ by the Pre-miRNA 92b in the Presence of 100 mM K^+

(A) DMS structure mapping of pre-miRNA 92b after the folding of RNA in the presence of 100 mM K^+, 100 mM Li^+, and without any added salt. Gs that are in the PQS region (G9 to G23) are protected from the DMS modification in the presence of 100 mM K^+ but not in the 100 mM Li^+ or in the no added salt lanes.

(B) The bands were assigned using a radiolabeled ladder. RNase T1 structure mapping of pre-miRNA 92b with increased enzyme concentration (1U) shows the G tracts that are in the PQS region (G13 to G28) were still protected in the presence of 100 mM K^+, indicating the formation of GQ structure. G31 to G41 were less protected in the 100 mM K^+ due to the unwinding of the stem-loop. The bands were assigned according to a base hydrolysis ladder.

(C) The numbered G residues in the mfold predicted stem-loop structure of pre-miRNA 92b.

(A) and (B) follow the numbering shown in (C).

WT RNA in the presence and absence of K^+ (Figure 5A). In 100 mM Li^+, the Dicer cleavage pattern of Mut 2 was similar to that observed in 100 mM K^+ and no added salt lanes, indicating that the Mut 2 maturation is independent of the concentration and identity of the salt (Figure 5B). This also established that the Dicer cleavage activity is similar under both 100 mM K^+ and Li^+. Because the pre-miRNA 92b was body labeled, the band intensities did not directly represent the amount of RNA, as their radiolabeled cytosine incorporation varied, but for a given band, the intensity can be used to compare the amount of RNA among different lanes.

Densitometric analysis showed that in case of the WT RNA, mature miR-92b level was about 5-fold lower in the presence of K^+ compared with the level in the absence of K^+ (no added salt), confirming the impediment of Dicer activity by the GQ structure (Figure 5C). However, no significant difference in miR-92b level was observed in the presence or absence of K^+ in the case of Mut 2 RNA cleavage. These results collectively establish that the formation of GQ structure inhibits the Dicer-mediated maturation of miRNA 92b in vitro. Using the Mut 2 molecule, we have already demonstrated that a designed disruption of the GQ formation rescues the maturation even in the presence of 100 mM K^+. Thus, the equilibrium between canonical hairpin structure and the noncanonical GQ structure plays a regulatory role in maturation of miRNA 92b at the intracellular K^+ concentration.

Since pre-miRNAs were internally labeled (body labeled), a small number of bands besides the mature product were observed in the Dicer cleavage assay. The band just above the 22-nt-long matured product can be a variant (isomiR), which is commonly found in miRNA maturation (Figure 5A) (Ameres and Zamore, 2013; Neilsen et al., 2012). These isomiRs are typically one or more nucleotides longer at the 5′ or 3′ end of the mature miRNA (Guo and Chen, 2014). Interestingly, this isomiR was not clearly observed in case of Mut 2 RNA as the nucleotides adjacent to the cleavage site are mutated and that may have abolished the potential isomiR cleavage site (Figure 5A). A more prominent band between 40 and 50 nt was observed with both WT and Mut 2, which is most likely an intermediate that is often found due to incomplete digestion of long pre-miRNAs, especially when the recombinant Dicer enzyme is used in vitro (Figures 5A and 5B) (Koscianska et al., 2011; Starega-Roslan et al., 2011). Other less intense bands may be the remaining portions of the pre-miRNA cleavage as most of the generated fragments were radioactive.

GQ Structure Formation Inhibits In Vivo Maturation of Pre-miRNA 92b Resulting in Repression of Target Gene Knockdown

Our in vitro data strongly suggest the presence of an equilibrium between the GQ-containing structure and the canonical stem-loop structure at the physiologically relevant K^+ concentration. Furthermore, we have established that in vitro the GQ structure formation inhibits Dicer activity by a significant amount. Next, we assessed the effect of GQ on pre-miRNA 92b maturation in vivo by a Dual-Luciferase assay in HEK 293 cells. A 22 nt sequence which is complementary to the predicted miR-92b seed sequence (complementary to the miR-92b-3p mature

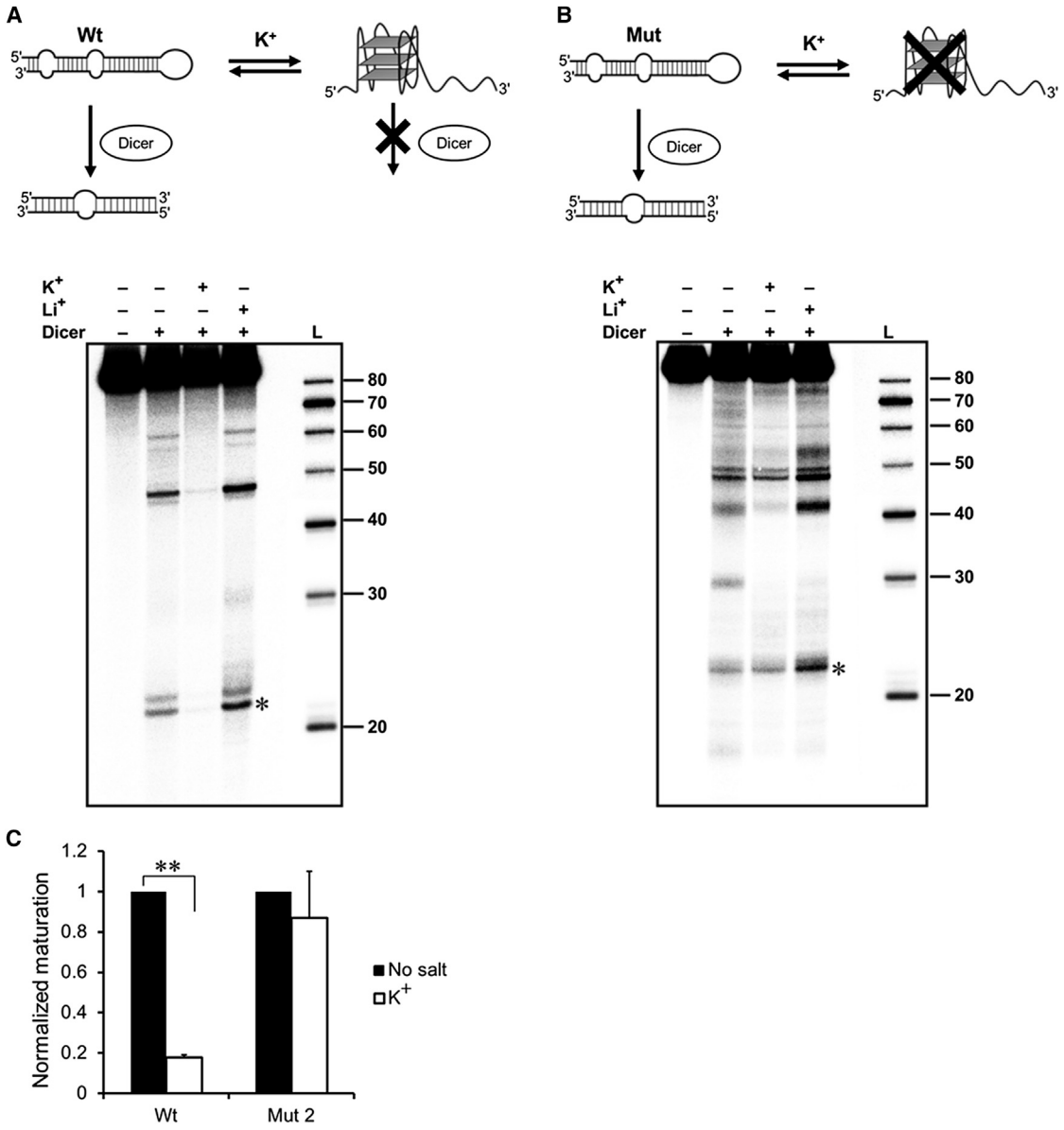

Figure 5. GQ Formation Inhibits Dicer-Mediated Maturation of Pre-miRNA 92b In Vitro

(A) In vitro Dicer assay of WT. Mature product (marked with *) was significantly lower in the presence of 100 mM K^+ but not with 100 mM Li^+ compared with the no salt lane. L, size ladder.

(B) In vitro Dicer assay of Mut 2, which does not have a PQS. No significant difference was obtained for the mature product (marked with *) between no salt, 100 mM K^+, and 100 mM Li^+. L, size ladder.

(C) The histogram showing the densitometric quantification of miR-92b maturation. Band intensities represent the relative level of mature miR-92b (marked with *). Five-fold higher inhibition of Dicer-mediated maturation was observed for WT in the presence of K^+ compared with the absence of K^+. Data represent mean values ± SEM, n = 3, $^{**}p < 0.001$.

sequence) was cloned within the 3′ UTR of the *Renilla* luciferase gene in psiCHECK-2 vector (Figure 6A). The firefly luciferase gene present in the same vector was used as a transfection control. Since mature miR-92b can knock down *Renilla* luciferase gene expression by binding to the incorporated seed sequence within its mRNA, relative luciferase activity (*Renilla* to firefly) would be inversely proportional to the amount of matured miR-92b present inside the cells. To control for the effect of any nonspecific knockdown of the reporter genes, an unmodified psiCHECK-2 vector without the seed sequence was utilized. In order to assess the effect of GQ formation, HEK 293 cells were cotransfected in separate wells with the in vitro transcribed WT or Mut 2 RNA and the psiCHECK-2 vector containing the seed sequence, respectively. In a control experiment, the WT RNA was cotransfected with the WT psiCHECK-2 vector instead of the one containing the seed sequence. Twenty-four hours post cotransfection, relative luciferase activities were measured and normalized to the control (Figure 6B). Relative luciferase activity

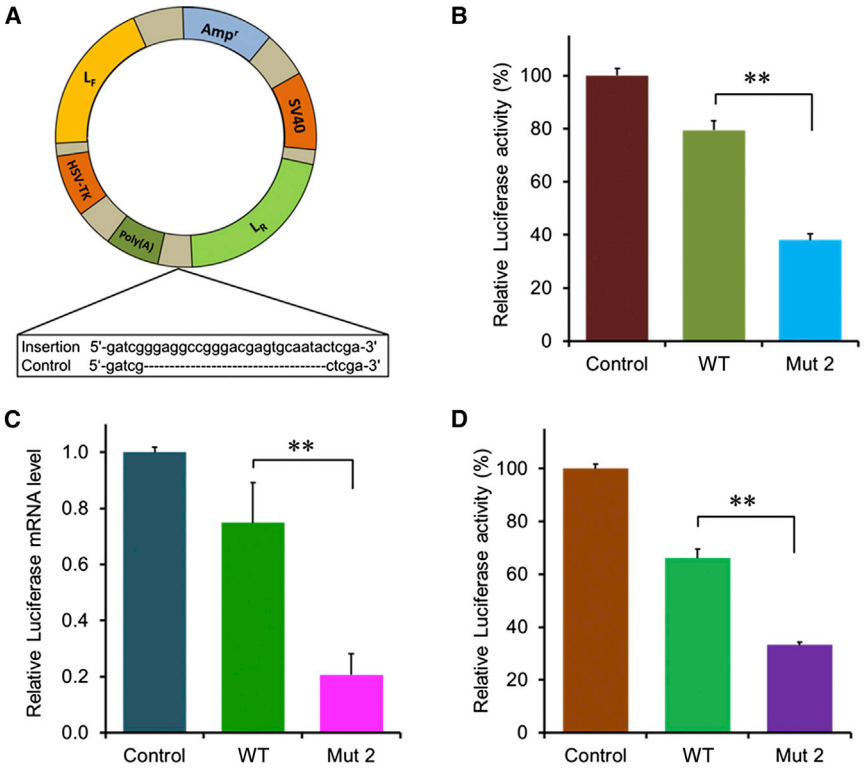

Figure 6. GQ Formation Inhibits Target Gene Knockdown by miR-92b In Vivo

(A) Plasmid map of psiCHECK-2 vector with the inserted seed sequence of miR-92b. A 22 nt complementary sequence to 3p-miR-92b mature sequence was inserted into the 3′ UTR of *Renilla* luciferase gene.

(B) The histogram representing the relative luciferase activities (*Renilla* to firefly) after the co-transfection of pre-miRNA 92b or Mut 2 with the plasmid vector in HEK 293 cells (n = 9 experiments, mean ± SEM, $^{**}p < 0.001$ by two-tail *t* test).

(C) *Renilla* mRNA level relative to firefly mRNA 24 hr after the cotransfection was validated by RT-qPCR (n = 3 experiments, mean ± SEM, $^{**}p < 0.05$ by two-tail *t* test).

(D) Relative luciferase activity 24 hr after the co-transfection of WT or Mut prefolded stem loops with the target vector (n = 4 experiments, mean ± SEM, $^{**}p < 0.05$ by two-tail *t* test).

with the Mut 2 was measured to be 2-fold lower than for the WT, suggesting that in the absence of GQ structure, there is increased pre-miRNA 92b maturation. It must be noted that both WT and Mut 2 pre-miRNA 92b will produce a similar mature sequence and any difference in target gene knockdown would reflect a difference in the level of maturation. Because the WT can form GQ structure, it would produce a smaller amount of mature miRNA 92b compared with the Mut 2. In order to assess that the knockdown is taking place at the mRNA level, luciferase mRNA levels were quantified 24 hr after the transfection by real-time qPCR (RT-qPCR). The normalized *Renilla* luciferase mRNA level was 2-fold lower when the cells were transfected with Mut 2 compared with the WT, indicating the GQ structure formation leads to reduced miRNA maturation, which in turn impedes the target gene knockdown at the mRNA level (Figure 6C). The reporter enzyme activity of the Mut 2 treated cells indicates that the target gene knockdown can be enhanced by abolishing the GQ structure of the pre-miRNA, as we established earlier that because of the lack of PQS, the Mut 2 should not form any GQ structure regardless of the intracellular K^+ concentration. The results discussed above strongly indicate that in vivo the pre-miRNA 92b maturation is inhibited by the GQ structure formation, which is a new mechanism for control of pre-miRNA maturation.

The Stem-Loop Structure Can Switch to the GQ Structure under Cellular Salt Conditions

Next, we intended to determine whether a prefolded stem-loop structure can be switched to the GQ-containing structural form under the cellular conditions. To investigate this, pre-miRNA was folded in the absence of K^+ to favor the stem-loop structure and the Dual-Luciferase assay was performed, as described in the previous section. Thus, before the transfection, both WT and Mut 2 RNAs were in the canonical stem-loop conformation. In vivo, if there is a stem-loop to GQ structural switch, then the level of target gene knockdown will be similar to what was reported in the previous section. Indeed, relative luciferase activity in the cells treated with Mut 2 was still 2-fold lower in comparison with the cells treated with WT, indicating the formation of GQ structure inside the cells (Figure 6D). This implies that the canonical stem-loop structure of pre-miRNA 92b switches to the GQ-containing form, which is resistant to Dicer cleavage activity in the cytosol, where average K^+ concentration is known to be at least 100 mM. Thus, it can be proposed that irrespective of the initial structure of pre-miRNA-92b, after the Drosha cleavage of the pri-miRNA, it would most likely resort to equilibrium with GQ structure once it is exported to the cytoplasm.

DISCUSSION

In this study, we have identified GQ as an alternative secondary structure to the canonical stem loop of the human pre-miRNA 92b, which directly affects its maturation. Our findings not only unravel a new mechanism that controls pre-miRNA maturation but also add a hitherto unknown layer of regulation to miRNA biogenesis. The existence of the PQS region among approximately 16% of the total number of human pre-miRNA stem loops suggests the importance of GQ structures in miRNA biogenesis. The list includes some of the most well-studied and biologically important pre-miRNAs.

The PQS in pre-miRNA 92b was found to be conserved among a wide range of species, validating the critical role of GQ structure. However, the challenge is formation of the GQ superseding the canonical stem-loop structure under the physiological conditions. The presence of monovalent and divalent cations can result in a reversible hairpin-GQ structural equilibrium within an RNA molecule, with GQ being the major conformer at physiologically relevant K^+ and Mg^{2+} concentrations (Bugaut et al., 2012).

Therefore, it was logical to test the feasibility of formation of the GQ structure over the pre-miRNA 92b canonical stem loop that is not a fully base-paired hairpin. Our data clearly showed (1) that the formation of GQ can unwind the entire stem-loop structure in the presence of physiologically relevant K^+ concentration and (2) the coexistence of a GQ-containing structure with the canonical stem loop. Pre-miRNA 92b can adopt three-tier GQs containing very short length loops (less than 2), which are characteristic of very stable GQ structures (Morris and Basu, 2009; Zhang et al., 2011). The pre-miRNA 92b stem-loop structure, which contains internal loops, mismatches, and bulges, unwinds due to the formation of a strong GQ structure in the presence of K^+ as was evident from the structure mapping results. The structural equilibrium between GQ and the stem loop is an entirely new phenomenon for pre-miRNA structures that can modulate the miRNA-mediated regulation of gene expression.

The structural equilibrium mentioned above can regulate the Dicer-mediated maturation of pre-miRNA 92b both in vitro and in vivo. Since the enzyme Dicer binds to a double-strand structure, an unwound stem loop containing the GQ should not be an efficient substrate for Dicer-mediated cleavage. In fact, the in vitro Dicer assay encountered a significant inhibition of dicing activity from the GQ structure formation. Since the coexistence was observed between the GQ and the stem-loop structure, one can speculate that the equilibrium would switch toward the stem-loop structure as it is being cleaved by the Dicer and should eventually reach 100% cleavage even in the presence of 100 mM K^+. However, such an equilibrium shift toward the stem loop and the consequent cleavage was not observed in the in vitro Dicer assay, suggesting the higher stability and the very low off rate of the GQ structure, which is consistent with the literature (Kim et al., 1991). Nevertheless, detailed kinetic analysis will be necessary to fully delineate the folding kinetics of the two structures.

The pre-miRNA may originate as a stem-loop structure after the Drosha-mediated maturation of long pri-miRNA hairpin, but our findings suggest that cytoplasmic K^+ concentration is sufficient to alter the stem-loop structure to the GQ form, which results in inhibition of the Dicer-mediated maturation. Thus, the inhibition of Dicer-mediated cleavage in vitro is physiologically relevant, a conclusion corroborated by the in cellulo reporter gene inhibition data. Although we showed that the pre-miRNA 92b maturation inhibition is most likely due to the GQ formation in concurrence with our in vitro data, more detailed experimentation will be needed to confirm the in vivo GQ formation of pre-miRNAs.

Several mechanisms of the regulation of Dicer-mediated maturation have been either shown or proposed, such as nuclear retention of pre-miRNA, binding of Lin-28 protein to pre-miRNA, and regulation of Dicer partner proteins (Ding et al., 2009; Ha and Kim, 2014). Here, we report the discovery of a new mechanism of regulation of Dicer-mediated maturation at the pre-miRNA structural level. In addition, our finding that the GQ structure regulates pre-miRNA maturation adds to the list of roles played by this noncanonical RNA structure.

Further studies are required to unravel the detailed mechanism of GQ-mediated regulation of miRNA maturation. It will be interesting to investigate the role of G-rich PQSs in other pre-miRNAs, which will help to establish the generality of the mechanism. Moreover, structural details of Dicer binding to the GQ structure need to be elucidated to generate information about why the GQ-containing pre-miRNAs are resistant to Dicer-mediated cleavage. Several proteins have been found to bind with RNA GQs and modulate the role of GQ structure in RNA processing and translation (Bugaut and Balasubramanian, 2012; Millevoi et al., 2012). Therefore, it is plausible that under certain circumstances, some proteins may bind to the GQ structure and destabilize it to increase the pre-miRNA 92b maturation. Another explanation might be that the equilibrium is fast enough and thus the GQ structure may control the rate of Dicer cleavage, rather than completely inhibit it, under the in vivo conditions. However, additional in vivo experiments are required to understand the detailed mechanism of how the pre-miRNA maturation is regulated by the equilibrium between the GQ and stem-loop structures inside the cells under different conditions.

Although our in vitro data, especially the native gel electrophoresis, showed that the stem-loop coexists with the GQ structure even in the presence of K^+ ions, we observed a significant decrease in reporter gene expression in the presence of WT pre-miRNA 92b in vivo where the K^+ is presumably present at a level sufficient for GQ formation. Since the intracellular K^+ concentration is known to be maintained more or less constant, the upregulation of GQ-containing pre-miRNAs under certain disease conditions may involve a GQ unwinding protein, as discussed above. However, further investigations are needed in order to unravel such regulation in vivo.

SIGNIFICANCE

We showed the presence of GQ structure in pre-miRNA 92b, which exists in equilibrium with the canonical stem-loop structure in vitro and most likely in the cytosol. This equilibrium regulates the maturation of pre-miRNA 92b, as the GQ-containing structure was shown to impede the Dicer-mediated maturation both in vivo and in vitro. Therefore, the GQ structure can play a pivotal role to keep the mature miR-92b cellular concentration at the basal level. This is essential for normal cellular functions as miR-92b knocks down many important genes, including tumor suppressor genes. The findings in the report expand our current understanding of the regulation of pre-miRNA maturation in general and begin to delineate modulation of the maturation process at the RNA structure level.

EXPERIMENTAL PROCEDURES

General Methods

Diethyl dicarbonate-treated autoclaved nanopure water was used to prepare all the solutions and buffers. All DNA oligonucleotides were purchased from Integrated DNA Technologies (IDT) and were purified by running on a denaturing polyacrylamide gel. Concentrations of all RNAs and DNAs were determined based on their UV absorbance values at 260 nm by using a NanoDrop ND-1000 spectrophotometer.

Plasmids, Restriction Digestion, and Site-Directed Mutagenesis

Details of plasmid generation, procedures for restriction digestion, and site-directed mutagenesis are described in the Supplemental Experimental Procedures.

RNA Preparation and 5′ End Labeling of the Purified RNA

Details for RNA preparation are given in the Supplemental Experimental Procedures.

RNase T1 Structure Mapping

The 5′ end radiolabeled RNA was folded by heating to 95°C for 5 min and cooled to room temperature in the presence of 100 mM K^+, 100 mM Li^+, or in the absence of any salt. Folded RNAs were subjected to RNase T1 (0.2 or 1 units, Ambion) digestion for 2 min at 37°C. The reactions were terminated by heating to 95°C for 2 min with an equal volume of 2× urea loading buffer that contained 7 M urea. Details on further analysis of the samples are provided in the Supplemental Experimental Procedures.

Dimethyl Sulfate Structure Mapping

Previously published protocols (Peattie, 1979) with minor changes were followed (details are provided in the Supplemental Experimental Procedures).

Gel Mobility Shift Assay

End-labeled (5′) RNAs were folded as described above and run on a 12% native polyacrylamide gel for 7 hr, 20 W, 4°C, and the running buffer was circulated frequently. The gel was dried on Whatman filter paper and the image was obtained as described above.

CD Melting Studies

RNAs were folded as described above and the CD melting curves were obtained using a Jasco J-810 spectropolarimeter. Melting curves were recorded by monitoring the ellipticity at 263.5 nm at 0.5°C intervals from 25°C to 95°C with 20°C/hr melting rate and 2.5 μM RNA. The minimum points in the first derivative curves of CD melting were recorded and average temperatures of three repeated experiments were reported as the melting temperatures.

Internal Labeling of RNA and In Vitro Dicer Assay

RNAs were transcribed by in vitro transcription as described above except a 6 μM final concentration of radioactive [α-^{32}P]CTP (PerkinElmer) was added to the transcription mixture for the body labeling. Radioactive transcripts were purified and precipitated as described previously. Purified pre-miRNAs were folded as described above and incubated with 10 mM Tris-HCl, 2 mM $MgCl_2$, 100 mM KCl or LiCl, 10 mM NaCl and 0.5 units of Turbo Dicer enzyme (Genlantis). The assay was performed by incubating the mixture at 37°C for 40 min, and the reaction was stopped by adding Dicer stop buffer (Genlantis). An equal volume of 2× urea loading buffer was added to the reaction mixtures and the products were run on a 10% denaturing PAGE for 70 min. The gel was dried on Whatman paper and exposed to a phosphorimager screen overnight. The gel images were visualized as described above.

Cell Culture and Cotransfection

Details of the cell culture are given in the Supplemental Experimental Procedures. Prefolded stem-loop structures or GQ structures of pre-miRNA (50 ng) were cotransfected with inserted or control psiCHECK-2 vectors (100 ng) and 0.5 μl of Lipofectamine 2000 (Life Technologies) to HEK 293 cells grown in 200 μl of medium.

Dual-Glo Luciferase Assay

After 24 hr from the cotransfection, *Renilla* and firefly luciferase activity were measured by Dual-Glo Luciferase Assay according to the manufacturer's protocol. Relative luciferase activity (*Renilla* to firefly) was calculated and normalized to the control.

Quantitative RT-PCR Assay

Details for the quantitative RT-PCR assay are given in the Supplemental Experimental Procedures.

SUPPLEMENTAL INFORMATION

Supplemental Information includes four figures, two tables, and Supplemental Experimental Procedures and can be found with this article online at http://dx.doi.org/10.1016/j.chembiol.2014.12.013.

AUTHOR CONTRIBUTIONS

S.B. supervised all aspects of the project. S.B. and G.M. designed the experiments. A.D. cloned the reporter gene vector and transcribed RNA for the thermal melting studies. G.M. performed the experiments and analyzed the data with the help of S.B. S.B. and G.M. wrote the manuscript.

ACKNOWLEDGMENTS

We thank Dr Kristian Baker (Case Western Reserve University) for valuable comments on the manuscript. We also thank the members of Basu Lab for the critical discussions during the preparation of the manuscript and the course of the project. We acknowledge Aparna Venkataraman (posthumous) for her contribution in the plasmid design and the initial bioinformatics studies. This work was supported by funding from Kent State University to S.B. and G.M. was partially funded by a research award from the GSS at Kent State University.

Received: November 10, 2014
Revised: December 11, 2014
Accepted: December 29, 2014
Published: January 29, 2015

REFERENCES

Aldaz-Carroll, L., Tallet, B., Dausse, E., Yurchenko, L., and Toulmé, J.-J. (2002). Apical loop-internal loop interactions: a new RNA-RNA recognition motif identified through in vitro selection against RNA hairpins of the hepatitis C virus mRNA. Biochemistry *41*, 5883–5893.

Ameres, S.L., and Zamore, P.D. (2013). Diversifying microRNA sequence and function. Nat. Rev. Mol. Cell Biol. *14*, 475–488.

Arora, A., Dutkiewicz, M., Scaria, V., Hariharan, M., Maiti, S., and Kurreck, J. (2008). Inhibition of translation in living eukaryotic cells by an RNA G-quadruplex motif. RNA *14*, 1290–1296.

Bartel, D.P. (2004). MicroRNAs: genomics, biogenesis, mechanism, and function. Cell *116*, 281–297.

Bernstein, E., Caudy, A.A., Hammond, S.M., and Hannon, G.J. (2001). Role for a bidentate ribonuclease in the initiation step of RNA interference. Nature *409*, 363–366.

Borchert, G.M., Lanier, W., and Davidson, B.L. (2006). RNA polymerase III transcribes human microRNAs. Nat. Struct. Mol. Biol. *13*, 1097–1101.

Bugaut, A., and Balasubramanian, S. (2012). 5′-UTR RNA G-quadruplexes: translation regulation and targeting. Nucleic Acids Res. *40*, 4727–4741.

Bugaut, A., Murat, P., and Balasubramanian, S. (2012). An RNA hairpin to G-quadruplex conformational transition. J. Am. Chem. Soc. *134*, 19953–19956.

Campbell, N., and Neidle, S. (2012). G-Quadruplexes and metal ions. In Interplay between Metal Ions and Nucleic Acids, A. Sigel, H. Sigel, and R.K.O. Sigel, eds. (Dordrecht: Springer), pp. 119–134.

Chen, X., and Yan, G.-Y. (2014). Semi-supervised learning for potential human microRNA-disease associations inference. Sci. Rep. *4*, 5501.

Darnell, J.C., Jensen, K.B., Jin, P., Brown, V., Warren, S.T., and Darnell, R.B. (2001). Fragile X mental retardation protein targets G quartet mRNAs important for neuronal function. Cell *107*, 489–499.

Denli, A.M., Tops, B.B., Plasterk, R.H., Ketting, R.F., and Hannon, G.J. (2004). Processing of primary microRNAs by the microprocessor complex. Nature *432*, 231–235.

Di Leva, G., Garofalo, M., and Croce, C.M. (2014). MicroRNAs in cancer. Annu. Rev. Pathol. *9*, 287.

Ding, X.C., Weiler, J., and Grosshans, H. (2009). Regulating the regulators: mechanisms controlling the maturation of microRNAs. Trends Biotechnol. *27*, 27–36.

Feng, Y., Zhang, X., Graves, P., and Zeng, Y. (2012). A comprehensive analysis of precursor microRNA cleavage by human Dicer. RNA *18*, 2083–2092.

Friedman, R.C., Farh, K.K.-H., Burge, C.B., and Bartel, D.P. (2009). Most mammalian mRNAs are conserved targets of microRNAs. Genome Res. *19*, 92–105.

Griffiths-Jones, S. (2004). The microRNA registry. Nucleic Acids Res. *32*, D109–D111.

Griffiths-Jones, S., Saini, H.K., van Dongen, S., and Enright, A.J. (2008). miRBase: tools for microRNA genomics. Nucleic Acids Res. *36*, D154–D158.

Gu, S., Jin, L., Zhang, Y., Huang, Y., Zhang, F., Valdmanis, P.N., and Kay, M.A. (2012). The loop position of shRNAs and pre-miRNAs is critical for the accuracy of Dicer processing in vivo. Cell *151*, 900–911.

Guo, L., and Chen, F. (2014). A challenge for miRNA: multiple isomiRs in miRNAomics. Gene *544*, 1–7.

Ha, M., and Kim, V.N. (2014). Regulation of microRNA biogenesis. Nat. Rev. Mol. Cell Biol. *15*, 509–524.

Hesse, M., and Arenz, C. (2014). MicroRNA maturation and human disease. In miRNA Maturation, C. Arenz, ed. (New York: Springer), pp. 11–25.

Hutvágner, G., McLachlan, J., Pasquinelli, A.E., Bálint, É., Tuschl, T., and Zamore, P.D. (2001). A cellular function for the RNA-interference enzyme Dicer in the maturation of the let-7 small temporal RNA. Science *293*, 834–838.

Jayaraj, G.G., Pandey, S., Scaria, V., and Maiti, S. (2012). Potential G-quadruplexes in the human long non-coding transcriptome. RNA Biol. *9*, 81–86.

Kikin, O., D'Antonio, L., and Bagga, P.S. (2006). QGRS Mapper: a web-based server for predicting G-quadruplexes in nucleotide sequences. Nucleic Acids Res. *34*, W676–W682.

Kim, J., Cheong, C., and Moore, P.B. (1991). Tetramerization of an RNA oligonucleotide containing a GGGG sequence. Nature *351*, 331–332.

Koscianska, E., Starega-Roslan, J., and Krzyzosiak, W.J. (2011). The role of Dicer protein partners in the processing of microRNA precursors. PLoS One *6*, e28548.

Krol, J., Sobczak, K., Wilczynska, U., Drath, M., Jasinska, A., Kaczynska, D., and Krzyzosiak, W.J. (2004). Structural features of microRNA (miRNA) precursors and their relevance to miRNA biogenesis and small interfering RNA/short hairpin RNA design. J. Biol. Chem. *279*, 42230–42239.

Kumari, S., Bugaut, A., Huppert, J.L., and Balasubramanian, S. (2007). An RNA G-quadruplex in the 5′ UTR of the NRAS proto-oncogene modulates translation. Nat. Chem. Biol. *3*, 218–221.

Kypr, J., Kejnovská, I., Renčiuk, D., and Vorlíčková, M. (2009). Circular dichroism and conformational polymorphism of DNA. Nucleic Acids Res. *37*, 1713–1725.

Lee, Y., Ahn, C., Han, J., Choi, H., Kim, J., Yim, J., Lee, J., Provost, P., Rådmark, O., and Kim, S. (2003). The nuclear RNase III Drosha initiates microRNA processing. Nature *425*, 415–419.

Lee, Y., Kim, M., Han, J., Yeom, K.H., Lee, S., Baek, S.H., and Kim, V.N. (2004). MicroRNA genes are transcribed by RNA polymerase II. EMBO J. *23*, 4051–4060.

Li, Y., Li, L., Guan, Y., Liu, X., Meng, Q., and Guo, Q. (2013). MiR-92b regulates the cell growth, cisplatin chemosensitivity of A549 non small cell lung cancer cell line and target PTEN. Biochem. Biophys. Res. Commun. *440*, 604–610.

Ma, E., Zhou, K., Kidwell, M.A., and Doudna, J.A. (2012). Coordinated activities of human Dicer domains in regulatory RNA processing. J. Mol. Biol. *422*, 466–476.

MacRae, I.J., Zhou, K.H., Li, F., Repic, A., Brooks, A.N., Cande, W.Z., Adams, P.D., and Doudna, J.A. (2006). Structural basis for double-stranded RNA processing by Dicer. Science *311*, 195–198.

MacRae, I.J., Zhou, K., and Doudna, J.A. (2007). Structural determinants of RNA recognition and cleavage by Dicer. Nat. Struct. Mol. Biol. *14*, 934–940.

Martadinata, H., and Phan, A.T. (2013). Structure of human telomeric RNA (TERRA): stacking of two G-quadruplex blocks in K+ solution. Biochemistry *52*, 2176–2183.

Millevoi, S., Moine, H., and Vagner, S. (2012). G-quadruplexes in RNA biology. Wiley Interdiscip. Rev. RNA *3*, 495–507.

Morris, M.J., and Basu, S. (2009). An unusually stable G-quadruplex within the 5′-UTR of the MT3 matrix metalloproteinase mRNA represses translation in eukaryotic cells. Biochemistry *48*, 5313–5319.

Morris, M.J., Negishi, Y., Pazsint, C., Schonhoft, J.D., and Basu, S. (2010). An RNA G-quadruplex is essential for cap-independent translation initiation in human VEGF IRES. J. Am. Chem. Soc. *132*, 17831–17839.

Nass, D., Rosenwald, S., Meiri, E., Gilad, S., Tabibian-Keissar, H., Schlosberg, A., Kuker, H., Sion-Vardy, N., Tobar, A., Kharenko, O., et al. (2009). MiR-92b and miR-9/9*are specifically expressed in brain primary tumors and can be used to differentiate primary from metastatic brain tumors. Brain Pathol. *19*, 375–383.

Neidle, S., and Balasubramanian, S. (2006). Quadruplex Nucleic Acids. (Cambridge: Royal Society of Chemistry).

Neilsen, C.T., Goodall, G.J., and Bracken, C.P. (2012). IsomiRs–the overlooked repertoire in the dynamic microRNAome. Trends Genet. *28*, 544–549.

Park, J.E., Heo, I., Tian, Y., Simanshu, D.K., Chang, H., Jee, D., Patel, D.J., and Kim, V.N. (2011). Dicer recognizes the 5′ end of RNA for efficient and accurate processing. Nature *475*, 201–205.

Peattie, D.A. (1979). Direct chemical method for sequencing RNA. Proc. Natl. Acad. Sci. USA *76*, 1760–1764.

Ruby, J.G., Jan, C.H., and Bartel, D.P. (2007). Intronic microRNA precursors that bypass Drosha processing. Nature *448*, 83–86.

Sand, M. (2014). The pathway of miRNA maturation. In miRNA Maturation, C. Arenz, ed. (New York: Springer), pp. 3–10.

Sengupta, S., Nie, J., Wagner, R.J., Yang, C., Stewart, R., and Thomson, J.A. (2009). MicroRNA 92b controls the G1/S checkpoint gene p57 in human embryonic stem cells. Stem Cells *27*, 1524–1528.

Starega-Roslan, J., Krol, J., Koscianska, E., Kozlowski, P., Szlachcic, W.J., Sobczak, K., and Krzyzosiak, W.J. (2011). Structural basis of microRNA length variety. Nucleic Acids Res. *39*, 257–268.

Sundquist, W.I., and Heaphy, S. (1993). Evidence for interstrand quadruplex formation in the dimerization of human immunodeficiency virus-1 genomic RNA. Proc. Natl. Acad. Sci. USA *90*, 3393–3397.

Winter, J., and Diederichs, S. (2011). MicroRNA biogenesis and cancer. In MicroRNA and Cancer, W. Wu, ed. (New York: Springer), pp. 3–22.

Winter, J., Jung, S., Keller, S., Gregory, R.I., and Diederichs, S. (2009). Many roads to maturity: microRNA biogenesis pathways and their regulation. Nat. Cell Biol. *11*, 228–234.

Wu, Z.B., Cai, L., Lin, S.J., Lu, J.L., Yao, Y., and Zhou, L.F. (2013). The miR-92b functions as a potential oncogene by targeting on Smad3 in glioblastomas. Brain Res. *1529*, 16–25.

Zhang, A.Y., Bugaut, A., and Balasubramanian, S. (2011). A sequence-independent analysis of the loop length dependence of intramolecular RNA G-quadruplex stability and topology. Biochemistry *50*, 7251–7258.

Zuker, M. (2003). Mfold web server for nucleic acid folding and hybridization prediction. Nucleic Acids Res. *31*, 3406–3415.

